

# Jahrestagung Assemblée Annuelle

Donnerstag, 3. Mai 2018 - Jeudi, 3 Mai 2018  
Auditorium Ettore Rossi  
Inselspital, Universitätsspital Bern  
3010 Bern

**SBMS**

The Swiss Bone and Mineral Society



**SVGO**

Schweizerische Vereinigung gegen die Osteoporose

**ASCO**

Association Suisse contre l'Ostéoporose

## Inhalt

### Short Communications

#### 1. Abstracts preclinical

- A 57 Z. Arabpour et al.: Influence of polymeric adjuvants on the properties of Platelet Rich Plasma gel
- A 57 L. Bourgoin et al.: Opg-Fc attenuates insulin-resistance and muscle weakness in a mouse model of diabetoporosis (Ppar $\beta$  KO)
- A 58 W. Baumgartner et al.: Biomimetic Cartilage/ Bone Interface
- A 58 R. Cabra et al.: The role of iron in development and activity of osteoclasts
- A 58 M. Gerbaix, S. Ferrari: Anabolic stimuli prevent the decline of bone formation associated with long-term exposure to sclerostin-neutralizing antibodies
- A 59 G. Monaco et al.: Chondrogenic culture media supplemented with high molecular weight hyaluronan to mimic healthy synovial fluid of the human knee joint
- A 60 B. Gatenholm et al.: Bone and cartilage mapping in human osteoarthritic knees
- A 60 M. Hildebrand et al.: Early prediction of healing outcome in a large bone defect rodent model via microCT
- A 61 C. Thouverey et al.: Osteoblast-specific ablation of p38 $\alpha$  MAPK signaling blocks bone formation in RANKL-stimulated bone turnover

- A 61 C. Thouverey et al.: Postnatal suppression of platelet-derived growth factor receptor signaling in osteoblasts increases bone mass in mice
- A 61 E. Wehrle et al.: The effect of individualized cyclic mechanical loading on the remodeling phase of fracture healing as assessed by time-lapsed in vivo imaging

#### 2. Abstracts clinical

- A 62 E. Biver et al.: Evaluation of radius microstructure and areal bone mineral density improves fracture prediction in postmenopausal women
- A 62 N. Bonnet et al.: Denosumab improves muscle function and glucose homeostasis
- A 63 T. Chevalley et al.: More frequent and more sustain osteoporosis treatment after fragility vertebral fractures when introduced early in inpatients than delayed in outpatients
- A 63 W. S. Enns-Bray et al.: Classification of hip fractures in elderly women in the AGES Reykjavik Study cohort using biofidelic finite element models
- A 64 D. E. Schenk, P.K. Zysset: Fast versus accurate estimation of Colles' fracture load of the distal radius by homogenized finite element analysis based on low- and high-resolution HR-pQCT
- A 64 S. Sebastian et al.: Potential of whole body vibration therapy to increase bone strength in adolescents with idiopathic scoliosis
- A 65 K. Simon et al.: Local in vivo assessment of human distal radius fractures by time-lapse HR-pQCT

## SHORT COMMUNICATIONS

### 1. Preclinical

#### Influence of polymeric adjuvants on the properties of Platelet Rich Plasma gel

Z. Arabpour<sup>1,2</sup>; J. Keller<sup>1</sup>; T. Serra<sup>1</sup>; M. Alini<sup>1</sup>; D. Eglin<sup>1</sup>; S. Verrier<sup>1</sup>

<sup>1</sup>AO Research Institut Davos, Davos Switzerland; <sup>2</sup>Dpt of Tissue Engineering, School of Advanced Technologies in Medicine, Tehran University of Medical Sciences, Iran

**Introduction:** Naturally rich in growth factors and cytokines (e.g. PDGF, VEGF), platelets play a pivotal role in wound healing. Platelet Rich Plasma (PRP) gel can be prepared from patient's own blood, has shown beneficial outcome in human and veterinary medicine (1) and can be used for cells and growth factors delivery (2–3). As biomaterial, PRP has poor mechanical properties and high degradation rate, reducing its stability and long-term effect. Here we investigate the mechanical properties and stability of PRP enriched with bioresorbable polymeric adjuvants.

**Methods:** PRP was prepared as previously described [4]. Briefly, Platelets concentrates from 3 donors (blood bank, Kantonspital Graubünden, Chur, CH) were centrifuged to obtain different concentrations of PRP: 10X, 15X and 50X higher than in the whole blood. Four polymeric adjuvants: Hyaluronic acid (HA), carboxymethyl cellulose (CMC), gelatin and polyvinyl alcohol (PVA) were added respectively to different PRP concentrations; and the jellification of PRP induced by addition of 2.5, 5 or 10U thrombin. Rheological (MCR, Anton Paar) and mechanical testing were performed, and the viscosity, elastic, viscous and Young moduli evaluated.

**Results:** An addition of 5U thrombin independently of the PRP concentrations leads to more stable gels in the absence and the presence of adjuvants. Addition of polymeric adjuvants increases the elastic and viscous moduli of PRP 15X and 50X, although with higher increase with PVA and gelatin in comparison to HA and CMC.

**Conclusions:** Here we show that the mechanical properties of PRP can be modulated by FDA approved polymeric adjuvants. Further experiments will assess their influence on the growth factors and cytokines release.

**References:** 1. Marques L et al. Platelets 2015; 2. Jalowiec J et al. TE Part C 2016; 3. Zahn J et al. Mediators Inflamm, Epub 2017; 4. Duttenhoefer F et al. eCM 2013.

#### Opg-Fc attenuates insulin-resistance and muscle weakness in a mouse model of diabetoporosis (Ppar KO)

L. Bourgoin<sup>1</sup>; B. Desvergne<sup>2</sup>; N. Bonnet<sup>1</sup>

<sup>1</sup>Division of Bone Diseases, Department of Internal Medicine Specialties, Geneva University Hospital & Faculty of Medicine, Geneva 14, Switzerland; <sup>2</sup>Center of Integrative Genomics, Genopode, Lausanne Faculty of Biology and Medicine CH-1015 Lausanne, Switzerland

RANKL/OPG are key regulators of osteoclastogenesis. We previously demonstrated that RANK is expressed in skeletal muscle and liver, and that mice overexpressing RANKL exhibit insulin resistance. We hypothesized that Opg-Fc is able to prevent bone loss, muscle weakness and insulin resistance in a diabetoporosis model. For this purpose, we treated Ppar $\beta$ <sup>-/-</sup> mice (KO) with Opg-Fc (4mg/kg/week) or vehicle (Veh) for 4 weeks. Muscle function was investigated by treadmill exercise, handgrip, microCT and infrared camera; gene expression by RT-qPCR and glucose handling by GTT and ITT. At 5 months of age, KO mice displayed a lower trabecular and cortical bone volume at the femur (-33% and -14% vs WT, p<0.05) as well as a lower muscle limb volume, limb temperature, maximal speed and force, -19%, -1.6%, -15% and -16% vs WT (p<0.05). GTT and ITT AUC were higher in KO, +38% and +8% vs WT (p<0.05). In the soleus, Glut1, Fabp4, CyclinD1, Pgc1 gene expression were downregulated whereas Myostatin and Fgf21 were upregulated (-29%, -22%, -20%, -7%, +33% and +172% vs. WT, p<0.05). In the liver, mRNA levels of gluconeogenic genes and stress markers like Pgc1, Fabp4, and Fgf21 were increased (+262%, +60% and +320% vs WT, p<0.01). Opg-Fc increased BV/TV and TbN (+107% and +40% vs Veh, all p<0.05). Opg-Fc increased the force, muscle volume and temperature of the limb (+6.7%, +12%, +1.8%, p<0.08). Moreover gene expression levels were normalized in soleus and liver. Opg-Fc decreased GTT and ITT AUC (-36.7% and -22.3% vs Veh, p<0.05) arguing for a restoration of the insulin sensitivity, confirmed by western blots in muscle and liver. In conclusion, Opg-Fc could rescue bone loss, muscle function, insulin-resistance and gluconeogenesis in a diabetoporosis model. Hence RANKL could play a central role in the concomitant development of osteoporosis, sarcopenia and diabetes.

**Keywords:** Diabetes, insulin resistance, muscle, RankL, Osteoprotegerin

## Biomimetic Cartilage/ Bone Interface

Walter Baumgartner<sup>1</sup>; Lukas Otto<sup>1</sup>; Samuel C. Hess<sup>2</sup>; Wendelin J. Stark<sup>2</sup>; Sonja Märsmann<sup>1,3</sup>; Maurizio Calcagni<sup>1</sup>; Paolo Cinelli<sup>3</sup>; Johanna Buschmann<sup>1</sup>

<sup>1</sup>Division of Plastic and Hand Surgery, University Hospital Zurich; <sup>2</sup>Institute for Chemical and Bioengineering, Department of Chemistry and Applied Biosciences, ETH Zurich; <sup>3</sup>Division of Trauma Surgery, University Hospital Zurich

**Introduction:** The interface between cartilage and bone is characterized by a gradient of calcium phosphate phases that decline in content from bone towards cartilage. Adipose-derived stem cells are able to differentiate into chondrocytes and osteoblasts, offering the option to use one single cell source for tissue engineering of a biomimetic cartilage/ bone interface.

**Methods:** We used an electrospun poly-lactic-co-glycolic acid (PLGA) mesh with incorporated amorphous calcium phosphate nanoparticles in different weight percentages, having a gradient from 30%, 20%, 10% and 0% towards the cartilage mimicking side of the biomimetic interface. The materials were seeded with human adipose-derived stem cells (ASCs) and either cultivated under static conditions or under dynamic conditions in a perfusion bioreactor without any further supplementation of the culture medium. After a total of four weeks, quantitative RT-PCR was performed for eleven relevant genes, including typical marker genes for osteo- and chondrogenesis, but also for adipo- and angiogenesis. In addition, histology and immunohistochemistry was performed to address cell density, proteoglycans and glycosaminoglycans.

**Results:** Under static conditions, the presence of amorphous calcium phosphate nanoparticles did not have any impact on osteo- and chondrogenesis related genes – only CD31 (and endothelial marker gene) was upregulated in the presence of nanoparticles compared to pure PLGA. In contrast, under dynamic conditions, ASCs exhibited an increased expression of chondrogenic marker gene Sox9 towards the cartilage mimicking side. In addition, ASCs showed an increased expression of osteogenic marker gene osteocalcin towards the bone mimicking side. The results found on the gene level were supported by findings on the protein level.

**Conclusion:** We conclude that amorphous calcium phosphate nanoparticles incorporated in electrospun PLGA meshes influence the differentiation behaviour of human ASCs. Electrospun meshes with gradients of nanoparticles may act as promising cartilage/bone interfaces when cultivated under perfusion in a bioreactor system.

## The role of iron in development and activity of osteoclasts

Romina Cabra<sup>1,2,3</sup>; Mark Siegrist<sup>1</sup>; Silvia Dolder<sup>1</sup>; Willy Hofstetter<sup>1,2</sup>

<sup>1</sup>Bone Biology & Orthopaedic Research, Department of clinical research; <sup>2</sup>Swiss National Centre of Competence in Research, NCCR TransCure; <sup>3</sup>Graduate School for Cellular and Biomedical Sciences

**Introduction:** Iron is an essential microelement. Divalent Metal Transporter (DMT1) is a membrane transporter involved in the

iron uptake and maintenance of iron homeostasis. In previous experiments, it has been demonstrated that DMT1 transcripts were upregulated during osteoclastogenesis. To elucidate the role of DMT1 and iron uptake in osteoclasts (OC), an osteoclast-specific DMT1-ko mouse model was generated using the Cre/lox system, where TRAP promoter drives Cre expression. Furthermore, an in vitro iron uptake assay for osteoclasts was developed.

**Methods:** Bone morphometry of DMT1(OC)fl/flCre+ lumbar vertebrae (L3-L5) was assessed by microCT. To evaluate the efficiency of DMT1 ko, levels of DMT1 transcripts were determined in mixed and homogeneous DMT1(OC)fl/flCre+ OC populations by RT-PCR. The effects of DMT1 deficiency on OC development, activity, and survival were assessed. To investigate the kinetics of iron uptake, mature osteoclasts pretreated ± iron chelator desferoxamine (DFO) were incubated for up to 2 hours with <sup>55</sup>Fe-Transferrin.

**Results:** Trabecular thickness of L5 vertebral secondary spongiosa was decreased by 20% in DMT1(OC)fl/flCre+ male mice. The levels of DMT1 transcripts were decreased in OC grown from progenitor cells from both DMT1(OC)fl/flCre+ male (70%) and female (30%) mice when compared with Cre- controls. No significant effects were detected on OC development, activity and survival. In vitro iron deprivation significantly upregulates the transcripts encoding TfR1 (90%) and DMT1 (30%) in OC. Consequently, iron uptake in OC/DFO was significantly increased (35%) compared to OC w/o DFO.

**Conclusion:** The efficiency of the osteoclasts-specific DMT1 ko is sex-dependent. The decrease in DMT1 transcripts in DMT1(OC)fl/flCre+ male mice causes a decrease in the trabecular thickness of lumbar vertebrae. However, in vitro the survival, development and activity of osteoclasts was not affected. In vitro iron deprivation leads to a significant upregulation of both TfR1 and DMT1 transcripts in OC and consequently to an increase in iron uptake.

## Anabolic stimuli prevent the decline of bone formation associated with long-term exposure to sclerostin-neutralizing antibodies

Maude Gerbaix<sup>1</sup>; Serge Ferrari<sup>1</sup>

<sup>1</sup>University Geneva Hospital (hug) / Faculty Of Medicine (unige), Genève, Suisse

Sclerostin inhibition by neutralizing Ab (Scl-Ab) in animals and humans leads to a massive increase, followed by a drastic downregulation, of predominantly modeling-based bone formation (1). Several mechanisms have been proposed, including upregulation of Sost and Dkk1, and/or exhaustion of osteoblast precursor pool. We hypothesized that the bone forming response to Scl-Ab could be maintained by anabolic stimuli known to both downregulate Sost expression and promote Sost-independent bone formation.

Four month-old mice received Scl-Ab (50 mg/kg/w) or vehicle for 7 weeks. At week 4, axial compression was applied on

the left tibia (16N to Scl-Ab treated mice, 12N to Veh mice, at 0.1 Hz, 7 min, 2 days/week) for 3 weeks. A Subgroup of mice concomitantly received PTH (40 µg/kg/d). Bone formation was evaluated by serum P1NP and microstructure by micro-CT.

In response to Scl-Ab, P1NP peaked at 2 weeks and returned to veh levels by 4 weeks. Scl-Ab maximally increased trabecular bone volume fraction (BV/TV) at distal femur and vertebrae (+159%, +187% respectively vs Veh;  $p < 0.01$ ) and cortical thickness (Ct.Th) at femur (+37% vs Veh;  $p < 0.01$ ) by 4 weeks with no significant gain thereafter. PTH administration from week 4 further increased BV/TV at femur (+16% vs Scl-Ab alone,  $p < 0.05$ ) and at vertebrae (+20.37% vs Scl-Ab alone;  $p < 0.05$ ), but not Ct.Th. Loading increased tibia BV/TV in AbScl group (+14% vs nonloaded tibia;  $p < 0.05$ ) and in AbScl+PTH group (+49% vs nonloaded tibia,  $p < 0.05$ ). Loading also increased tibia Ct.Th in AbScl group (+19% vs nonloaded tibia;  $p < 0.05$ ) and in AbScl+PTH group (+12% vs nonloaded tibia;  $p < 0.05$ ).

In summary, continuous exposure to Scl-Ab leads to a rapid decline of bone formation, which can be rescued by both intermittent PTH and mechanical loading. These observations suggest that lining cells and osteoblasts precursors are still responsive and could be further stimulate by Sost independent mechanisms.

**References:** 1. Ominsky MS, Brown DL, Van G, et al. Differential temporal effects of sclerostin antibody and parathyroid hormone on cancellous and cortical bone and quantitative differences in effects on the osteoblast lineage in young intact rats. *Bone* 2015; 81: 380–391.

## Chondrogenic culture media supplemented with high molecular weight hyaluronan to mimic healthy synovial fluid of the human knee joint

**Graziana Monaco**<sup>1,2</sup>; **Mauro Alini**<sup>1</sup>; **Alicia J. El Haj**<sup>2</sup>; **Martin J. Stoddart**<sup>1,2</sup>

<sup>1</sup>AO Research Institute Davos, Switzerland; <sup>2</sup>Institute for Science & Technology in Medicine, Keele University, United Kingdom

**Introduction:** Strategies for cartilage repair often expose the regenerative exogenous cells to synovial fluid and its components. High molecular weight hyaluronan (HA) which is found in healthy synovial fluid is known to have a biological function whilst also affecting osmolality (1). In this study, we hypothesize that a chondrogenic medium containing high molecular weight HA may better recapitulate the rheological and biological features of the healthy synovial fluid present in the patients' intra-articular joints. Thus, our aim is to investigate chondrogenic culture media which contains physiological concentrations of sodium hyaluronate to more closely resemble the chemical composition, the biologic activity and the viscosity of healthy synovial fluid. Specifically, we investigated the effect of the HA on the chondrogenesis of human mesenchymal stem cells (hMSCs) that would be present in a traumatic defect after marrow stimulation techniques such as microfracture.

**Methods:** Cylindrical porous polyurethane (PU) scaffolds were prepared as previously described (2). hMSCs were isolated from human bone marrow aspirates obtained with full ethical approval, suspended at passage 3 in a fibrinogen-thrombin-solution and evenly seeded at a cell density of  $5 \times 10^6$  cells/scaffold. Scaffolds were fed with four different media for 28 days of culture. Control medium was serum free DMEM supplemented with 1% ITS<sup>+</sup>, 1% Pen/Strep, 1% non-essential amino acid, 50µg/ml ascorbate-2-phosphate, 5µM ε-amino-caproic acid (EACA),  $10^{-7}$ M dexamethasone (HA<sup>-</sup> TGFβ<sup>-</sup>). This media was further supplemented with 10 ng/mL TGFβ1 (HA<sup>-</sup> TGFβ<sup>+</sup>) or with 0.2% HA (HA<sup>+</sup> TGFβ<sup>-</sup>) or both (HA<sup>+</sup> TGFβ<sup>+</sup>). HA of 1,800 kDa was added to simulate synovial fluid concentration and viscosity under normal conditions (2.3 mg/ml) (3, 4). HA of 1,000kDa was also added into the scaffolds of one group at 0.02% (HAS TGFβ<sup>+</sup>). Total RNA was isolated from the constructs with TRI reagent and TaqMan reverse transcription and Real time qPCR were performed to investigate gene expression. Total DNA content and sulphated glycosaminoglycans (GAG) were measured spectrofluorometrically following reaction with DMMB pH 1.5. All samples containing HA were blanked with blank containing HA. Safranin O/Fast Green staining was performed to identify proteoglycan and collagen-rich areas. All experiments were performed on three independent donors, with measurements being conducted in triplicate or quintuplicate.

**Results:** Gene expression among the groups was comparable, with the notable exception of a downregulation of the hypertrophic marker collagen X in the presence of HA (HA<sup>+</sup> TGFβ<sup>+</sup>) in the first two weeks of culture compared to (HA<sup>-</sup> TGFβ<sup>+</sup>). Total GAG synthesized in samples supplemented with HA alone was consistently higher if compared with the control medium that was not supplemented (HA<sup>-</sup> TGFβ<sup>-</sup>). There was significant GAG production within the first week in all samples supplemented with HA, both in the presence and absence of active TGFβ. The findings described, and the general trend of the GAG level released into the media along 28 days of chondrogenic culture were consistent in all three different donors. ECM deposition was particularly evident in HAS TGFβ<sup>+</sup> histology sections.

**Discussion:** Our results demonstrate that the addition of HA to the culture medium has a positive effect on the intrinsic capacity of hMSCs to produce ECM, especially in the early days of chondrogenesis. Additionally, exogenous HA may prevent up-regulation of the hypertrophic cartilage marker, Collagen X, that is normally induced by active TGFβ. Finally, since this work aim to better reproduce the real in-vivo intrarticular environment conditions, the new media developed can be also used as a chondrogenic differentiation media model for *in-vitro* or *ex-vivo* studies where hMSCs are involved.

**Significance/Clinical relevance:** *In-vitro* models aim to recapitulate *in vivo* conditions. In order to mimic more closely the *in vivo* physiology, current models need to be improved to reflect the complexity of the joint environment. Therefore, in the current climate of animal welfare and „3Rs“, more accurate *in-vitro*/*ex-vivo* models will be crucial to prevent in-vitro artefacts and to

enable more accurate prescreening of potential cartilage repair therapies.

**Acknowledgements:** Project funded by AO Research Institute, Davos, Switzerland.

**References:** 1. Avenoso et al. *Inflammation Research* 2017; 1–16. 2. Boissard et al. *Acta Biomaterialia* 2009; 5(9): 3316–3327. 3. Akmal M et al. *J Bone Joint Surg Br* 2005; 87: 1143–1149. 4. Balazs EA et al. *Arthritis Rheum* 1967; 10: 357–376.

## Bone and cartilage mapping in human osteoarthritic knees

Birgitta Gatenholm<sup>1</sup>; Carl Lindahl<sup>2</sup>; Mats Brittberg<sup>1,3</sup>; Vincent A. Stadelmann<sup>4</sup>

<sup>1</sup>Department of Orthopaedics, Sahlgrenska University Hospital, Gothenburg, Sweden; <sup>2</sup>Department of Clinical Chemistry and Transfusion Medicine, Sahlgrenska University Hospital, Gothenburg, Sweden; <sup>3</sup>Region Halland Orthopaedics, Kungsbacka Hospital, Kungsbacka, Sweden; <sup>4</sup>SCANCO Medical AG, Brüttisellen, Switzerland

**Introduction:** Osteoarthritis (OA) is the most common joint disease causing morbidity and disability in patients worldwide. OA is no longer considered an isolated cartilage disease but rather a whole joint disease where the subchondral bone plays an important role in pain and disease. In this study we have used  $\mu$ CT to characterize subchondral bone microarchitecture and EPIC  $\mu$ CT to analyze cartilage damage from patients with advanced OA.

**Experimental methods:** Ten tibial plateaus were retrieved from patients with advanced OA who underwent total knee arthroplasty (TKR) surgery at Sahlgrenska University Hospital Sweden, following a procedure approved by the local ethics committee. Directly post-operatively, the samples were photographed (► Fig. 1), and split to fit each half into a Ø7 cm sample holder. After removal of excess fluid the explants were wrapped in cling-film and scanned with a microCT scanner (uCT100 Scanco Medical, Brüttisellen, Switzerland) operated at 70kVp, 200uA, 500ms with a nominal resolution of 36 $\mu$ m. After the initial scan, the samples were immersed in a contrast agent (40%

Hexabrix 320, 60% PBS) at room temperature for various durations under slow agitation and then re-scanned.

**Image processing:** First bone and cartilage were segmented based on the specific x-ray absorptions. A distance transformation algorithm was used to reveal variations in cartilage thickness and defect areas (► Fig. 1). The cartilage surface of each condyle was manually contoured from the bone surface and the contour was projected to the cartilage. The CA content at equilibrium was computed from the ROI in the registered stained scan to estimate its quality from the sGAG content.

**Results and discussion:** In our sample, cartilage thickness correlated spatially with subchondral bone thickness and density. To our knowledge, this is the first study using human OA tibial plateaus with EPIC  $\mu$ CT. Such samples have a high scientific value, because of their rarity but the sampling is biased since only diseased patients will have TKR. Mapping cartilage and bone quality spatially within sample by combining  $\mu$ CT of bone with EPIC  $\mu$ CT of cartilage the 3D model of osteochondral region enables studying the progress of the disease in the available samples.

## Early prediction of healing outcome in a large bone defect rodent model via microCT

Maria Hildebrand<sup>1</sup>; Marietta Herrmann<sup>1,2</sup>; Fabian Gieling<sup>1</sup>; Dominic Gehweiler<sup>1</sup>; Sophie Verrier<sup>1</sup>; Mauro Alini<sup>1</sup>; Stephan Zeiter<sup>1</sup>; Keith Thompson<sup>1</sup>

<sup>1</sup>AO Research Institute Davos, Davos, Switzerland; <sup>2</sup>IZKF Research Group Tissue Regeneration in Musculoskeletal Diseases, Orthopedic Center for Musculoskeletal Research, University Würzburg, Germany

Pre-clinical models are essential for understanding both the biological and biomechanical aspects of bone healing, as well as to develop treatments for critical bone defects. Since most of the current models rely on the sheer size of the osteotomy to impede healing – so called critical-size defects – they do not truly reflect the complex situation of delayed unions. Therefore, establishing a pre-clinical model with a predictable healing outcome will not only enhance our understanding of the biological and biomechanics of bone healing, they will also aid the development and testing of future intervention strategies.

Femoral osteotomies (gap sizes: 2mm and 1mm) were created in female, skeletally mature Fischer rats following fixation with either a 2mm or 1.25mm PEEK plate (RISystem), will full ethical approval (TVB 14E/2016), yielding 4 experimental groups (n=7/group). MicroCT analysis was performed post-operatively, after 2, 3, 4 weeks and biweekly until 14 weeks. Biomechanical testing of the different plate designs was also performed for axial bending, 4-point bending and torsional stiffness.

The 1.25mm plate resulted in improved healing rates in both 1mm and 2mm defect sizes compared to the 2mm plate (7/14 healed compared to 3/14 healed within 14 weeks, respectively), indicating the negative impact of overly stiff fixation for effective healing. In general, the larger 2mm defect size demonstrates

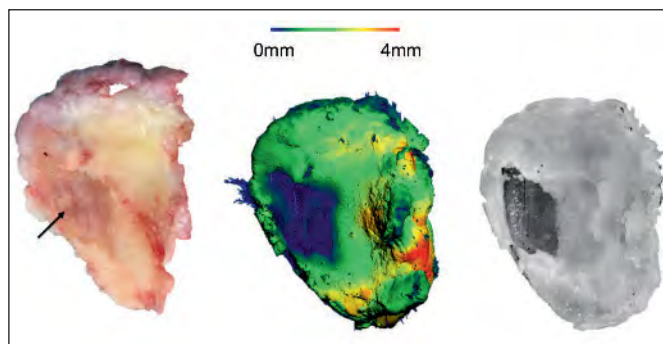


**Fig. 1** (left) photograph of a condyle with cartilage defect (arrow). (Center) thickness map of cartilage reveals the defect but shows normal thicknesses elsewhere. (Right) sGAG density map.

poorer healing responses compared to the 1mm defect, as demonstrated by only 3/14 animals bridging the 2mm defect whereas 7/14 animals bridged the 1mm defect within 14 weeks. Interestingly, healing outcome can be accurately predicted by 4 weeks in 2mm defects but not in 1mm defects.

In conclusion, we can accurately predict the healing outcome of a large bone defect by 4 weeks. This model system of delayed union will thereby allow the future testing of early intervention strategies aimed at stimulating effective healing responses in non-healing animals.

### Osteoblast-specific ablation of p38 MAPK signaling blocks bone formation in RANKL-stimulated bone turnover

**Cyril Thouverey, Joseph Caverzasio, Serge Ferrari**

Service of Bone Diseases, Department of Internal Medicine Specialties, University Hospital of Geneva

Osteoporosis is the consequence of a failure of osteoblasts in re-filling bone cavities dug out by osteoclasts despite the existence of various signals that couple bone resorption to bone formation. Osteoblastic p38 $\alpha$  MAPK signaling pathway positively regulates bone formation but can be diverted from its anabolic activity in condition of bone loss induced by estrogen withdrawal. We hypothesized that p38 $\alpha$  MAPK is important in osteoblasts to couple bone resorption to formation. To test this hypothesis, 8-week-old female mice lacking p38 $\alpha$  in osteoblasts (*Ocn-Cre;p38 $\alpha$ <sup>fl/fl</sup>*) and their control littermates (*p38 $\alpha$ <sup>fl/fl</sup>*) were treated with 2 subcutaneous injections of 1 mg/kg recombinant RANKL in a 24-hour interval to stimulate bone remodeling or its vehicle solution. Their bone microarchitecture and their serum levels of bone resorption/formation markers were measured 3 and 14 days after the second injection of RANKL. RANKL injections did not affect cortical bone mass but induced loss of 80% of initial trabecular bone mass in mice of both genotypes within 3 days. *p38 $\alpha$ <sup>fl/fl</sup>* mice recovered 87% of their trabecular bone 14 days after RANKL injections while *Ocn-Cre;p38 $\alpha$ <sup>fl/fl</sup>* mice only recovered 36% of trabecular bone mass ( $p \leq 0.01$ ). As expected, 3 days after RANKL injections serum levels of tartrate-resistant acid phosphatase (TRAP) were elevated by 2.3-fold ( $p \leq 0.05$ ) and carboxy-terminal collagen crosslinks (CTX) by around 4-fold ( $p \leq 0.05$ ) in mice of both genotypes. Interestingly, at the same time-point, serum levels of aminoterminal propeptide of type I collagen (PINP) and osteocalcin were increased by respectively 2.2 ( $p \leq 0.01$ ) and 1.5-fold ( $p \leq 0.05$ ) in *p38 $\alpha$ <sup>fl/fl</sup>* mice but not in *Ocn-Cre;p38 $\alpha$ <sup>fl/fl</sup>* mice. In conclusion, our results show that bone formation in RANKL-stimulated bone turnover is impaired in mice lacking p38 $\alpha$  MAPK signaling in osteoblasts, and thus suggest that this kinase is a mediator of the coupling reaction linking bone resorption to formation.

### Postnatal suppression of platelet-derived growth factor receptor signaling in osteoblasts increases bone mass in mice

**Cyril Thouverey, Joseph Caverzasio, Serge Ferrari**

Service of Bone Diseases, Department of Internal Medicine Specialties, University Hospital of Geneva

Platelet-derived growth factor (PDGF) BB, which can act through both PDGF receptors (PDGFR)  $\alpha$  and  $\beta$ , is secreted by pre-osteoclasts in the bone microenvironment. Osteoblast lineage cells highly express PDGFR $\alpha$  and PDGFR $\beta$ , suggesting that PDGF-BB/PDGFR signaling may directly regulate osteoblast development and function. To investigate the role of PDGFR $\alpha/\beta$  in osteoblast biology, we generated mice lacking PDGFR $\alpha$ , PDGFR $\beta$  or both receptors in osteoblast lineage cells by breeding mice expressing the Cre recombinase under the control of an inducible Osterix promoter (*Osx-Cre*) with mice harboring floxed genes encoding PDGFR $\alpha$  or PDGFR $\beta$ . The Cre expression and consequent *Pdgfra* or/and *Pdgfrb* inactivation were induced at 1.5 month of age by stopping doxycycline treatment. The bone phenotype of control (*Osx-Cre*),  $\Delta$ *Pdgfra*,  $\Delta$ *Pdgfrb* and  $\Delta$ *Pdgfra;\Delta**Pdgfrb* were assessed by micro-computed tomography at 4.5 months of age. All mutant mice were of normal weight and size.  $\Delta$ *Pdgfra* mice did not exhibit any bone phenotype.  $\Delta$ *Pdgfrb* mice did not show any difference in cortical bone geometry but displayed increased trabecular bone volume at proximal tibiae (+26%,  $p \leq 0.03$ ) associated with elevated number of trabeculae (+16%,  $p \leq 0.04$ ).  $\Delta$ *Pdgfra;\Delta**Pdgfrb* mice exhibited a further increase in trabecular bone volume at proximal tibiae (+50%,  $p \leq 0.02$ ) and augmented cortical bone volume at tibial midshafts (+24%,  $p \leq 0.04$ ). In conclusion, suppression of PDGFR signaling in osteoblasts increases trabecular and cortical bone mass in mice.

### The effect of individualized cyclic mechanical loading on the remodeling phase of fracture healing as assessed by time-lapsed *in vivo* imaging

**Esther Wehrle<sup>1</sup>; Graeme R. Paul<sup>1</sup>; Duncan C. Betts<sup>1</sup>; Gisela A. Kuhn<sup>1</sup>; Ralph Müller<sup>1</sup>**

<sup>1</sup>Institute for Biomechanics, ETH Zurich, Zurich, Switzerland

**Introduction:** Mechanical conditions are crucial for fracture healing. To understand the underlying mechanisms, refined *in vivo* loading models are needed. Here, we combine time-lapsed *in vivo* imaging with individualized loading protocols based on strain distribution in the fracture callus determined by finite element analysis (FEA). The study specifically focuses on the effect of cyclic mechanical loading on the remodeling phase of fracture healing.

**Methods and Results:** Female 20-week-old mice ( $n=20$ ) received a femur osteotomy and were scanned weekly (week 0–7; vivaCT 40, Scanco Medical, Brüttsellen, Switzerland). Scans were registered consecutively and morphometric indices computed. From week 4–7, individualized cyclic loading (8–16N, 10Hz, 3000cycles; 3x/week; controls – 0N) was applied based on computed strain distribution in the callus using an animal-specific

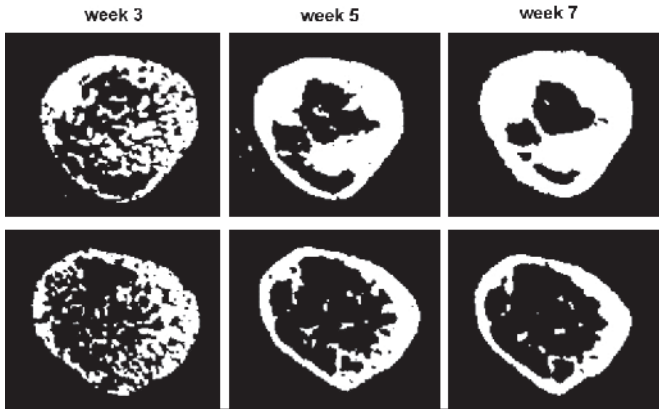


**Fig. 1** Representative thresholded ( $395 \text{ mg HA/cm}^3$ ) images of callus cross-sections from the loading (top) and control (bottom) group.

FEA approach: A micro-CT image of the mouse femur defect is acquired, pre-processed using a threshold-binning approach to create a multi-density finite-element mesh and submitted for FEA (Swiss National Supercomputing Centre). Full-bone and cross-section images containing the highest strains are generated and a strain histogram is plotted. This information allows matching of strain distributions to a particular mouse, to determine optimised load amplitude.

After bridging of the femur defect, the real-time FEA based approach allowed determination of initial loads (8N-12N), weekly load-scaling and matching of strain distribution in the callus for the 4 week loading period. At the end of study, loaded animals had 151% more bone in the defect compared to controls (► Fig. 1) with a significantly larger fraction of highly mineralized bone ( $BV_{645/395} \text{ week7: } 91 \pm 2 \text{ vs. } 84 \pm 2\%$ ).

**Conclusion:** This novel loading model combined with time-lapsed *in vivo* micro-CT shows the remodeling phase to be responsive to animal-specific cyclic mechanical loading with significantly improved callus properties. Complementing this study with local cell-type-specific gene and protein expression analyses will enable understanding of the mechano-molecular regulation of fracture healing.

## 2. Short communications clinical

### Evaluation of radius microstructure and areal bone mineral density improves fracture prediction in postmenopausal women

**Emmanuel Biver<sup>1</sup>; Claire Durosier-Izart<sup>1</sup>; Thierry Chevalley<sup>1</sup>; Bert van Rietbergen<sup>2</sup>; René Rizzoli<sup>1</sup>; Serge Ferrari<sup>1</sup>**

<sup>1</sup>Division of Bone Diseases, Geneva University Hospitals and Faculty of Medicine, University of Geneva, Switzerland; <sup>2</sup>Department of Biomedical Engineering, Eindhoven University of Technology, Eindhoven, Netherlands

A majority of low-trauma fractures occurs in subjects with only moderate decrease of areal bone mineral density (aBMD), i.e.

osteopenia, assessed by dual-energy X-ray absorptiometry (DXA), or low fracture probability assessed by FRAX. We investigated whether peripheral bone microstructure and estimated strength improve the prediction of incident fractures beyond central DXA and FRAX. In this population-based study of 740 postmenopausal women (age  $65.0 \pm 1.4$  years) from the Geneva Retirees Cohort (ISRCTN registry 11865958), we assessed at baseline cortical (Ct) and trabecular (Tb) volumetric bone mineral density (vBMD) and microstructure by peripheral quantitative computed tomography (HR-pQCT), bone strength by micro-finite element analysis, aBMD and trabecular bone score (TBS) by DXA, and FRAX fracture probability. Eighty five low-trauma fractures occurred in 68 women over a follow-up of  $5.0 \pm 1.8$  years. Tb and Ct vBMD and microstructure predicted incident fractures, independently of each other and of femoral neck (FN) aBMD and FRAX (with  $BMD \pm TBS$ ). However, the associations were markedly attenuated after adjustment for ultra-distal radius aBMD (same bone site). The best discrimination between women with and without fracture was obtained at the radius with total vBMD, the combination of a Tb with a Ct parameter, or with failure load which improved the area under the curve (AUC) for major osteoporotic fracture when added to FN aBMD ( $0.760 \text{ vs } 0.695$ ,  $p=0.022$ ) or to FRAX-BMD ( $0.759 \text{ vs } 0.714$ ,  $p=0.015$ ). The replacement of failure load by ultra-distal aBMD did not significantly decrease the AUC ( $0.753$ ,  $p=0.747$  and  $0.750$ ,  $p=0.509$ , respectively). In conclusion, peripheral bone microstructure and strength improve the prediction of fractures beyond central DXA and FRAX, but are partially captured in aBMD measured by DXA at the radius. Since HR-pQCT is not widely available for clinical purposes, assessment of ultra-distal radius aBMD by DXA may meanwhile improve fracture risk estimation.

### Denosumab improves muscle function and glucose homeostasis

**N. Bonnet; E Biver; L Bourgoïn; T Chevalley; M. Hars; A. Trombetti; S Ferrari.**

Division of Bone Diseases, Geneva University Hospitals and Faculty of Medicine, Geneva, Switzerland.

RANKL is a key regulator of osteoclastogenesis, but is also expressed in skeletal muscle and liver. Objective: Investigate if RANKL inhibitor Denosumab (Dmab) modifies muscle mass/function, and glucose homeostasis in mice overexpressing human RANKL (huRANKL). HuRANKL mice were treated with Dmab ( $10 \text{ mg/kg/week}$ ) or vehicle (Veh) for 4 weeks. Muscle function was investigated by running and handgrip test and glucose by GTT, ITT and EH clamp. In addition, 18 postmenopausal women treated for osteoporosis with Dmab and 20 treated by bisphosphonates (BPs) were evaluated by DXA and handgrip. They were matched to 55 controls for age ( $65.0 \pm 1.4$  years), BMI, BMD and fracture. HuRANKL mice have severe osteoporosis and lower maximal speed and limb force, respectively  $-41\%$  and  $-11\%$  vs WT ( $p < 0.05$ ). Gastrocnemius

and soleus mass were lower (-29% and -57% vs WT,  $p < 0.05$ ) and liver mass higher (+16% vs WT,  $p < 0.05$ ). ITT AUC was higher, +31% vs WT ( $p < 0.05$ ) and GIR, an index of insulin sensitivity was lower (-24.6%,  $p < 0.05$ ). 2D[14C]-glucose incorporation indicate a lower glucose uptake in the soleus (-51.9% vs WT,  $p < 0.05$ ). Hepatic glucose production was higher (+133% vs WT,  $p < 0.05$ ). Dmab increases limb force (+34.7% vs Veh,  $p < 0.05$ ) and normalizes ITT (AUC  $464 \pm 25.1$  vs  $353.9 \pm 8.1$  in Dmab,  $p < 0.05$ ) and hepatic glucose production ( $4.3 \pm 3.2$  vs  $-6.2 \pm 2$  mg/kg/min in Dmab,  $p < 0.05$ ). In women, after  $3.0 \pm 1.5$  years of Dmab and  $2.5 \pm 1.8$  years of BPs, both treatments increase LSBMD (respectively  $+0.12 \pm 0.29$  g/cm<sup>2</sup> and  $+0.04 \pm 0.12$  g/cm<sup>2</sup>) compared to controls ( $-0.07 \pm 0.19$  g/cm<sup>2</sup>, both  $p < 0.05$ ). In contrast only Dmab increase appendicular lean mass and handgrip strength ( $+0.66 \pm 2.2$  kg,  $+3.22 \pm 10.0$  kg, respectively) whereas it decrease both in BPs ( $-0.06 \pm 0.39$  kg,  $-0.07 \pm 6.6$  kg, respectively) and controls ( $-0.36 \pm 1.03$  kg,  $-1.39 \pm 2.4$  kg, respectively, both  $p < 0.05$ ). In conclusion, overexpression of huRANKL causes bone loss, impairs muscle function and insulin sensitivity. Denosumab reversed these defects in mouse, but also had some positive effects on muscle function in osteoporotic women. Altogether these point towards a potentially new mechanism relating RANKL expression to fracture risk, i.e. not only by decreasing bone, but also muscle strength.

### More frequent and more sustain osteoporosis treatment after fragility vertebral fractures when introduced early in inpatients than delayed in outpatients

T. Chevalley<sup>1</sup>; H. Spechbach<sup>2</sup>; I. Fabreguet<sup>1</sup>; E. Saule<sup>1</sup>; M. Hars<sup>1</sup>; J. Stirnemann<sup>2</sup>; S. Ferrari<sup>1</sup>; R. Rizzoli<sup>1</sup>

<sup>1</sup>Division of Bone Diseases; <sup>2</sup>Division of General Internal Medicine, University Hospitals and Faculty of Medicine, Geneva, Switzerland

**Objective:** Patients identification and osteoporotic fracture secondary prevention through fracture liaison service (FLS) are presently osteoporosis standard care. More frequent and adequate treatment is ensured when introduced in FLS than upon recommendation to primary care physician (PCP). Whether higher prevalence of treatment is observed when initiated in inpatients than by recommendations to PCP for patients systematically searched for vertebral fracture in a service of general internal medicine is not known. We tested whether early management of inpatients with newly identified vertebral fractures leads to a higher percentage of patients with osteoporosis medication than delayed management in outpatients.

**Methods:** Patients over 60 years systematically searched for vertebral fractures by semi-quantitative visual grading on lateral chest and/or spinal radiographs at admission or during hospital stay in a general internal medicine ward were included either in phase 1 (outpatients care – recommendations to PCP on assessments and osteoporosis medications to be prescribed) or phase 2 (inpatient care – assessments and osteoporosis medication initiated in hospital). The percentage of patients under specific

osteoporosis treatment was evaluated by telephone-interview at 3 and 6 months.

**Results:** Patients included in phases 1 (84 with fracture out of 407 assessed, 21%;  $75.7 \pm 7.7$  years) and 2 (100/524, 19%;  $77.8 \pm 9.4$  years) were similar for gender, age, Charlson comorbidity index, prior fractures, FRAX score and grade 1 or  $\geq 2$  vertebral fractures prevalence. A specific osteoporosis medication was more often prescribed in phase 2 than in phase 1 at 3 (67 vs 19%,  $p < 0.001$ ) and 6 months (69 vs 27%,  $p < 0.001$ ). Percentage of patients still under treatment was higher in phase 2 than in phase 1 at 3 (52 vs 19%,  $p < 0.001$ ) and 6 months (54 vs 29%,  $p < 0.001$ ). Similar results were observed in patients with grade  $\geq 2$  vertebral fracture only. Length of stay and destination after discharge were not different between both phases.

**Conclusions:** This controlled study highlights that early patient assessment and osteoporosis treatment initiation during hospital stay rather than delayed management in outpatients, is a more efficacious strategy of secondary fracture prevention for oldest olds with newly detected vertebral fragility fractures, and that without difference in length of stay.

### Classification of hip fractures in elderly women in the AGES Reykjavik Study cohort using biofidelic finite element models

W. S. Enns-Bray<sup>1</sup>; H. Bahaloo<sup>2</sup>; I. Fleps<sup>1</sup>; Y. Pauchard<sup>3</sup>; E. Taghizadeh<sup>4</sup>; S. Sigurdsson<sup>5</sup>; T. Aspelund<sup>5</sup>; P. Büchler<sup>4</sup>; T. Harris<sup>6</sup>; V. Gudnason<sup>5</sup>; S. J. Ferguson<sup>1</sup>; H. Pálsson<sup>2</sup>; B. Helgason<sup>1,7</sup>

<sup>1</sup>ETH-Zürich, Zürich, Switzerland; <sup>2</sup>University of Iceland, Reykjavik, Iceland; <sup>3</sup>University of Calgary, Alberta, Canada; <sup>4</sup>University of Bern, Bern, Switzerland; <sup>5</sup>Icelandic Heart Association, Kopavogur, Iceland; <sup>6</sup>National Institute on Aging, MD, USA; <sup>7</sup>Reykjavik University, Reykjavik, Iceland

Clinical retrospective studies have reported limited improvements in hip fracture classification accuracy using finite element analysis (FEA), compared to conventional areal bone mineral density (aBMD) measurements. The aim of this study was to develop and investigate the accuracy of a novel FE modeling technique to improve the biofidelity of simulated impact loading from sideways falling.

The FE models in this study included the pelvis, lower extremities, and soft tissue that were morphed to shape based on subject anthropometrics. Hip fracture prediction based on aBMD and the FE models were compared in a retrospective study of 254 elderly female subjects from the AGES-Reykjavik study cohort. Subject fragility ratio (FR) was defined as the ratio between the ultimate forces of paired biofidelic models, one with linear elastic and the other with non-linear, bone material properties. The expected end-point value (EEV) was defined as the FR weighted by the probability of one sideways fall over five years, based on self-reported fall frequency at baseline. The change in maximum volumetric strain ( $\Delta$ MVS) was calculated between ultimate force and 90% post-ultimate force in order to

assess the extent of tensile tissue bone damage present in non-linear FE models.

After age-adjusted logistic regression, the area under the receiver-operator curve (AUC) was highest for  $\Delta$ MVS (0.72), followed by FR (0.71), aBMD (0.70), and EEV (0.67). The differences between FEA and aBMD based prediction models were not statistically significant. When subjects with no history of falling were excluded from the analysis, a statistically significant difference in AUC was detected between  $\Delta$ MVS (0.85) and aBMD (0.74). Multivariable linear regression suggested that the variance in maximum elastic femur force was best explained by femoral head radius, pelvis width, and greater trochanter soft tissue thickness ( $R^2=0.79$ ; RMSE=0.46 kN;  $p<0.005$ ).

In summary, weighting the hip fracture prediction models based on self-reported fall frequency did not improve the models' sensitivity, however excluding non-fallers led to significant differences between aBMD measurements and FEA predictors. These findings suggest that an accurate assessment of fall probability is necessary for accurately identifying individuals predisposed to hip fracture.

### Fast versus accurate estimation of Colles' fracture load of the distal radius by homogenized finite element analysis based on low- and high-resolution HR-pQCT

Denis E. Schenk<sup>1</sup>; Philippe K. Zysset<sup>1</sup>

<sup>1</sup>Institute for Surgical Technology and Biomechanics, University of Bern, Bern, Switzerland

Radius fractures often reveal an early onset of osteoporosis. A double section scanning protocol using HR-pQCT encompasses Colles' fracture site, which mechanical properties can be computed accurately using non-linear homogenized finite element (hFE) analysis. As processing time and reproducibility are important for clinical applications, the aim of this work was to compare the predictions of radial mechanical properties between fast, low resolution (LR:82 $\mu$ m) and accurate, high resolution (HR:61 $\mu$ m) hFE, with respect to experimental data.

In a previous study (1), the 20mm most distal section of 21 human cadaveric radii were scanned with HR-pQCT with LR and HR protocols. For assessment of stiffness and strength, they were dissected out and tested under compression up to failure. The fast LR hFE model is based on a single isotropic phase, while the accurate HR model distinguishes cortical and trabecular bone as two distinct bone phases with different fabric-based orthotropic material properties (► Fig. 1). Stiffness and ultimate

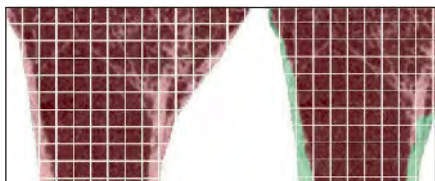


**Fig. 1**  
Fast, monophasic LR, isotropic (left) and accurate, two-phase HR, orthotropic (right) models.

load obtained from the FE analyses were individually fitted to the corresponding experimental results.

The non-linear hFE simulation achieved a coefficient of determination  $R^2=0.971$  (see=619N) and  $R^2=0.974$  (see=596N) for fast and accurate prediction of strength and  $R^2=0.873$  (8929N/mm) and  $R^2=0.900$  (see=8859N/mm) for prediction of stiffness, respectively. Mean total processing time per sample for image processing and FE analysis was approximately 4min for the fast and 60min for the accurate model.

The fast and accurate models achieved similar predictions of stiffness and strength. The additional processing time used for the accurate protocol doesn't significantly improve the results in view of clinical applications.

**References:** 1. Hosseini et al. Bone 2017; 97: 65–75.

### Potential of whole body vibration therapy to increase bone strength in adolescents with idiopathic scoliosis

Stephanie Sebastian<sup>1</sup>; Gianna Marano<sup>1</sup>; Yuk-Wai Wayne Lee<sup>2</sup>; Tsz-Ping Lam<sup>2</sup>; Ralph Müller<sup>1</sup>; and Patrik Christen<sup>1</sup>

<sup>1</sup>ETH Zurich, Institute for Biomechanics, Zurich, Switzerland; <sup>2</sup>The Chinese University of Hong Kong, Department of Orthopaedics & Traumatology, Hong Kong, China

**Introduction:** Adolescent idiopathic scoliosis (AIS) is a three-dimensional spinal deformity mainly affecting pubertal girls. It is associated with low bone mass as well as with inferior mechanical and abnormal bone structural properties, which might contribute to curve progression and increased risk of osteoporosis in adulthood. Pharmacological intervention for low bone mass during pubertal growth is lacking owing to unknown side and long-term effects. Our previous randomized clinical trial (RCT) showed that whole body vibration (WBV) was able to improve bone density parameters at the femoral neck and the lumbar spine for patients with AIS. However, it is still unclear if WBV is mechanically advantageous. The aim of the present study was to determine if WBV could have a positive effect on bone strength in AIS patients.

**Methods:** Baseline and 12-month follow-up high-resolution peripheral quantitative computed tomography (HR-pQCT) images of the distal tibia of 101 AIS females were used from a previous study. A treatment group of 54 participants stood on a low-magnitude, high frequency WBV-plate for 20 mins/day, 5 days/weeks for 12 months, whereas the remaining 47 participants served as controls. Bone tissue loading and bone strength were estimated using micro-finite element analysis. Local peak loading was assessed as the strain energy density (SED) value found at the 98th-percentile.

**Results:** The percent changes in bone strength and local peak loading between treatment and control groups were not statistically significant, which may be in part due to the large variation in patient's response to the WBV therapy. This is further supported by the smaller variation in percent changes in bone strength in the control group as compared to the treatment group.

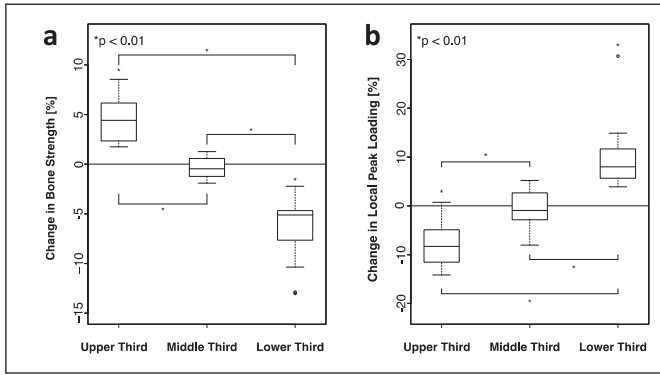


**Fig. 1** Boxplots showing the change in a) bone strength and b) local peak loading for the three treatment subgroups. Participants who experienced an increase in bone strength saw a decrease in local peak loading and vice versa. This demonstrates that some participants may benefit from WBV therapy whereas others may not.

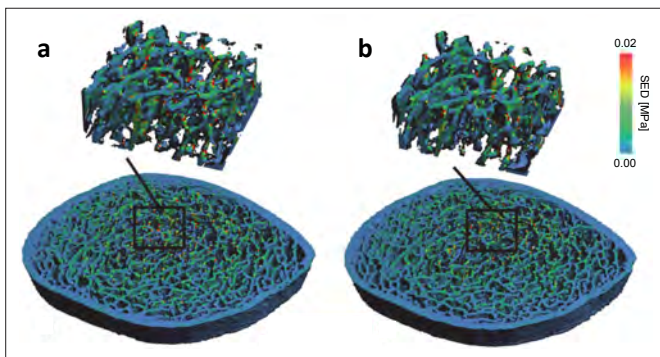


**Fig. 2** Local peak loading, as assessed with SED, in the distal tibia of an AIS patient in the upper third group at a) baseline and b) after receiving 12-month WBV therapy. This demonstrates an increase in bone strength and a decrease in local peak loading.

Treated patients with increased bone strength (upper third, n=18) revealed a significant ( $p < 0.01$ ) decrease of local peak loading where treated patients with decreased bone strength (lower third, n=18) showed an increase in local peak loading ( $p < 0.01$ ) (► Fig. 1). The decrease in local peak loading in subjects of the upper third group is apparent in the SED map (► Fig. 2). Linear regression models suggest the possible involvement of several factors, including cortical area ( $p = 0.0494$ ) and cortical thickness ( $p = 0.0732$ ) affecting the mechanical response to WBV therapy.

**Conclusion:** We conclude that WBV therapy could be beneficial to some AIS patients. Further investigation is required to determine influential factors for AIS candidates that would benefit from WBV therapy.

**Acknowledgements:** Authors acknowledge CPU time from the Swiss National Supercomputing Centre (CSCS) and funding from the Research Grants Council of Hong Kong (14135016).

## Local *in vivo* assessment of human distal radius fractures by time-lapse HR-pQCT

**Kerstin Simon**<sup>1</sup>; **Gianna Marano**<sup>2</sup>; **Michael Blauth**<sup>1</sup>; **Rohit Arora**<sup>1</sup>; **Ralph Müller**<sup>2</sup>; and **Patrik Christen**<sup>2</sup>

<sup>1</sup>University Hospital Innsbruck, Department of Trauma Surgery, Innsbruck, Austria; <sup>2</sup>ETH Zurich, Institute for Biomechanics, Zurich, Switzerland

**Introduction:** Bone fracture healing in patients is not well understood, e.g., the effects of mechanical loading, age, and osteoporosis are largely unknown. This is mainly due to the limited assessment of the healing process by clinical radiological parameters that do not allow to resolve the local changes in the tissue occurring during the healing process. With the advent of *in vivo* high-resolution peripheral quantitative computed tomography (HR-pQCT), it is now possible to assess the distal radius and tibia in great detail resolving individual trabeculae and thus the local tissue-level. Here, we present a time-lapse *in vivo* HR-pQCT imaging approach with the ultimate aim to study the healing of distal radius fractures at the local tissue-level over time.

**Methods:** Distal radius fracture patients treated conservatively by cast immobilisation are included while patients with previous or contralateral wrist injuries are excluded from the study. The study was approved by the Ethics Committee of the Medical University Innsbruck.

Time-lapse *in vivo* imaging is performed with a HR-pQCT system (XtremeCT II, Scanco Medical AG, Switzerland) with an effective energy of 68 kVp, a voxel size of 61 micrometres, beam intensity of 1470  $\mu$ A, integration time of 43 ms, and image matrix of 2304 x 2304 pixels. The effective radiation dose per measurement is below 5  $\mu$ Sv. Imaging is performed at baseline (week 1), 3 weeks, 5 weeks, 3 months, 6 months, and 12 months follow-up. The imaging process can be described as follows: The patient is positioned in an adjustable chair as comfortable as possible and is instructed to sit completely still. The forearm is placed in neutral position with flexed fingers in a special-purpose fixator (Cast, Scanco Medical AG, Switzerland) and secured with three tapes to avoid movement artefacts as much as possible. To generate comparable follow-up images of the same region, a reference line is attached to the cast on which the distal end of the metacarpals is placed.

According to an anterior-posterior scoutview of the distal end of the radius, the scanning region is defined in such a way that it includes the fracture region. By visual inspection, the distal border is defined in the middle of the articular surface. Starting from this position, a consecutive stack of 165 slices is scanned by the system. Depending of the fracture size, three to four stacks are imaged. No automated slice matching is used. These settings are saved as control files for view and reused in the next visit to gain replicable and overlapping scanning regions. As a control, the contralateral forearm is scanned using the same protocol but using only one stack as recommended by the manufacturer.

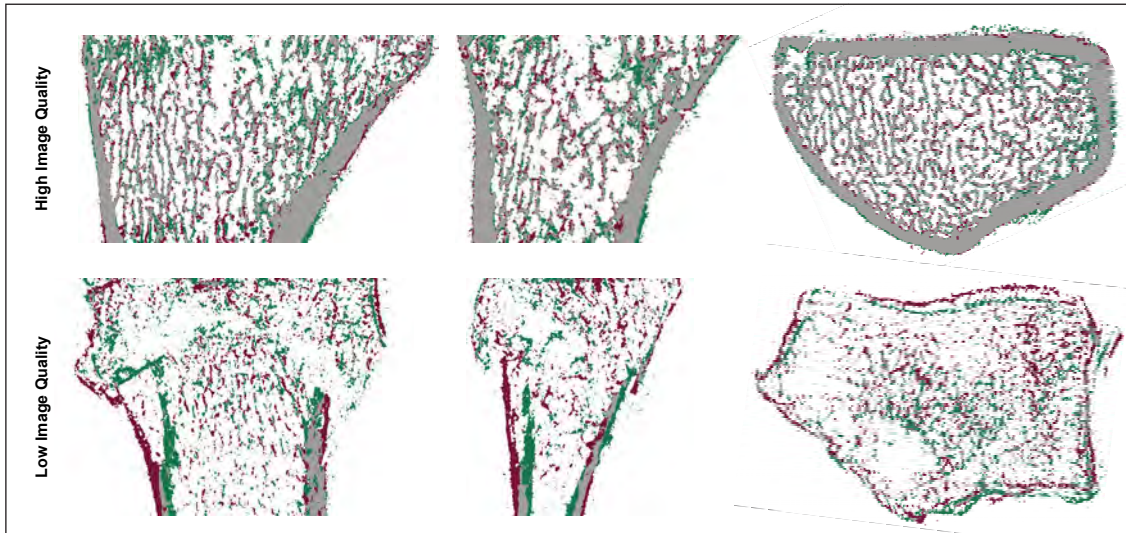


**Fig. 1** Local bone formation (green) and bone resorption (purple) occurring over three weeks of fracture healing based on high and low image quality HR-pQCT images.

To evaluate whether it is ultimately possible to study fracture healing at the local tissue-level, rigid image registration was used to align follow-up images and subtraction of the segmented images to determine local sites of bone formation and bone resorption.

**Results:** Within 6 months, 43 patients were recruited. Three of them already finished the 6-month assessment. Five patients did not finish the study due to missed control appointment because of medical reasons unrelated to the study (stroke and appendectomy) or lack of reachability. Distal radius fractures were generally located within 20 to 30 mm of the articular surface. Determining local bone formation and bone resorption revealed realistic outcomes with high image quality but was not possible for images with low image quality (► Fig. 1). Low image quality can be attributed to movement artifacts, extremely low bone density (osteoporotic bone), and fracture complexity. Movement arti-

facts were likely due to fracture instability and were age dependent where older patients had more difficulties to hold still. It is important to note that extremely low bone density was only observed in one case so far (T-scores of the spine = -3.2 and femur = -2.1), indicating that the presented imaging approach generates high quality images in the majority of the cases.

**Conclusion:** With the presented time-lapse *in vivo* HR-pQCT imaging of distal radius fractures it is potentially possible to assess fractures in patients at the level of individual trabeculae provided the patient is able to hold still during imaging and the bone density is not extremely low.

**Acknowledgements:** Funding from the Swiss National Science Foundation (Lead Agency, 320030L\_170205), German Research Foundation, and Austrian Science Fund for the DACH Fx Project is gratefully acknowledged.